A&A manuscript no.
(will be inserted by hand later)

Your thesaurus codes are:
03 (11.09.1 Maffei 2 11.09.4 13.19.1)

ASTRONOMY AND ASTROPHYSICS
July 10, 2000

Dense gas in nearby galaxies

XIV. Detection of hot ammonia in Maffei 2

Henkel, C.[1], **Mauersberger, R.**[2], **Peck, A.B**[1], **Falcke, H.**[1], **Hagiwara, Y.**[1]

[1] Max-Planck-Institut für Radioastronomie, Auf dem Hügel 69, D-53121 Bonn, Germany
[2] Instituto de Radioastronomía Milimétrica, Avda. Divina Pastora, 7NC, E-18012 Granada, Spain

Received date / Accepted date

Abstract. The (J, K) = (1,1), (2,2), (3,3), and (4,4) inversion lines of ammonia (NH_3) have been detected toward the nuclear 40″ sized bar of the nearby spiral galaxy Maffei 2. The relative intensities of the ammonia lines are characterized by a rotational temperature of 85 K. This is higher than rotational temperatures measured toward IC 342 and most Galactic Center clouds, implying kinetic temperatures $\gtrsim$100 K. Since the kinetic temperature of the gas is larger than that of the dust, NH_3 is tracing a particularly dense warm gas component that is heated by young massive stars, cloud-cloud collisions, or ion-slip heating in the nuclear starburst. The gas north of the nucleus (V_{LSR} = –80 km s^{-1}) is more highly excited than the gas further south (+6 km s^{-1}). This asymmetry might be related to pronounced morphological distortions that are observed in the north-eastern part of the galaxy.

Key words: Galaxies: individual (Maffei 2) – Galaxies: ISM – Galaxies: radio lines

1. Introduction

For the past decade, it has been possible to study the excitation of the molecular gas in external galaxies (e.g. Mauersberger & Henkel 1989; Mauersberger et al. 1990; Jackson et al. 1995; Hüttemeister et al. 1997; Paglione et al. 1997; Heikkilä et al. 1999; Mao et al. 2000). While the interpretation of CO emission often requires the application of complex models that incorporate temperature gradients at the surfaces of clouds, species like CS, HCN, or HC_3N trace higher density gas closer to the cloud cores and may thus be properly modeled with the standard 'Large Velocity Gradient' approach. Observed line intensity ratios of such high density tracers depend mostly on the number density $n(H_2)$, but also on the kinetic temperature T_{kin} of the gas. It is virtually impossible to disentangle these parameters, making observations of a molecule tracing exclusively temperature highly desirable.

Ammonia (NH_3) is such a molecule. With a single telescope-receiver configuration at 18–26 GHz, a large number of NH_3 inversion transitions can be measured, covering an enormous range of molecular excitation levels. These include the (J, K) = (1,1) to (4,4) inversion lines at 23, 65, 123, and 199 K above the ground state. Extragalactic ammonia was first detected in the (J, K) = (1,1) line toward the nearby face-on spiral IC 342 (Martin & Ho 1979). This was followed by detections of the (2,2), (3,3), and (4,4) lines (Ho et al. 1982, 1990; Martin & Ho 1986) that permitted a first estimate of the kinetic temperature of the dense nuclear gas in an external galaxy.

In view of the four ammonia lines observed toward IC 342 (the (6,6) line was also tentatively detected) it is surprising how little is known about ammonia in other external galaxies. Motivated by our unpublished detections of (J, K) = (1,1) and (2,2) emission in 1994 and by recent improvements in receiver sensitivity, baseline stability, and accessible bandwidth, we present a multilevel ammonia study of Maffei 2, an optically obscured barred spiral galaxy that is located behind the plane of the Milky Way at a distance of ∼2.5 Mpc (e.g. Karachentsev et al. 1997). High lower limits to the kinetic temperature of its dense nuclear gas are derived.

2. Observations

All data presented here were taken in March 2000, using the Effelsberg 100-m telescope of the MPIfR equipped with a dual channel K-band HEMT receiver. The system temperature was ∼220 K on a main beam brightness temperature scale; the beam size was ∼40″. The data were recorded using an autocorrelator with 8×256 channels and bandwidths of 80 MHz. The eight backends were configured in two groups of four, sampling data from both linear polarizations. Frequency shifts between the four backends representing a given linear polarization were adjusted in such a way that the (J, K) = (1,1) to (4,4) lines of ammonia could be measured simultaneously.

Send offprint requests to: C. Henkel

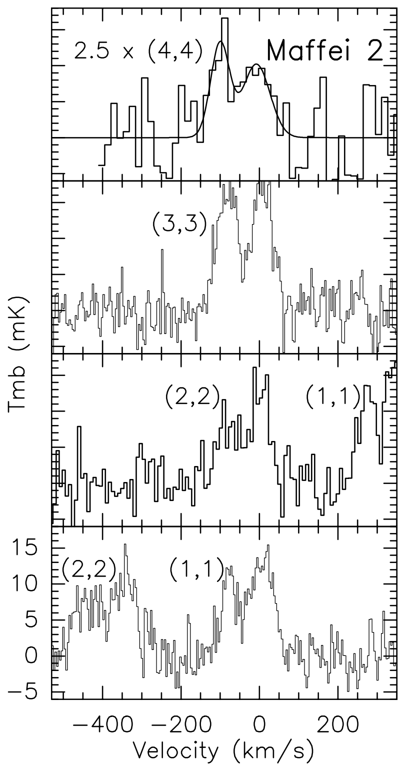

Fig. 1. NH_3 spectra towards Maffei 2 ($\alpha_{1950} = 2^{\mathrm{h}}\ 38^{\mathrm{m}}\ 08^{\mathrm{s}}.5$, $\delta_{1950} = +59^\circ\ 23'\ 24''$) after subtraction of linear baselines. Channel spacings are 3.9, 7.8, 3.9, and 15.7 km s^{-1} for the $(J,K) = (1,1)$ to (4,4) lines at 23694.496, 23722.631, 23870.130, and 24139.417 MHz, respectively. The NH_3 (4,4) spectrum, with the temperature scale multiplied by a factor of 2.5, is shown with a tentative gaussian decomposition.

The measurements were carried out in a dual beam switching mode (switching frequency 1 Hz) with a beam throw of 121$''$ in azimuth. Calibration was obtained by measurements of the radio continuum of W3(OH) and 3C 286 (for fluxes, see Baars et al. 1977; Mauersberger et al. 1988; Ott et al. 1994) and NH_3 spectra of Orion-KL and IC 342 (Martin & Ho 1986; Hermsen et al. 1988). We estimate an absolute calibration accuracy of ±10%. Relative calibration should be even more accurate, at the order of ±5%. Pointing errors as well as weather or elevation dependent gain variations affect all lines in a similar way; the calibration signal injected by a noise diode shows little frequency dependence and remains stable (within at least 5%) over the observed frequency interval. Spectral intensities were converted to a main beam brightness temperature ($T_{\rm mb}$) scale. Pointing was checked every hour on nearby continuum sources and was found to be stable to within 5–10$''$.

Table 1. Integrated line intensities ($\int T_{\rm mb} {\rm d}v$), Local Standard of Rest velocities ($V_{\rm LSR}$), full width to half power linewidths ($\Delta V_{1/2}$), and upper state column densities ($2{\cdot}N_{\rm u}(J,K) \sim N(J,K)$) for the (1,1) to (4,4) lines of ammonia towards Maffei 2. Line parameters were obtained from gaussian fits to the data. Errors in Cols. 3 and 4 are standard deviations from the fit; Cols. 2 and 5 also include a 10% uncertainty in absolute calibration (see Sect. 2).

Transition (J,K)	$\int T_{\rm mb}\,{\rm d}v$ K km s^{-1}	$V_{\rm LSR}$ km s^{-1}	$\Delta V_{1/2}$	$N_{\rm u}(J,K)$ 10^{12} cm^{-2}
(1,1)	0.527±0.080	–78±2	43±6	3.44±0.52
(1,1)	1.024±0.121	+6±2	70±5	6.69±0.78
(2,2)	0.694±0.122	–78±6	83±12	3.40±0.60
(2,2)	0.782±0.131	+5±4	66±10	3.83±0.63
(3,3)	1.127±0.131	–82±2	62±4	4.88±0.57
(3,3)	1.110±0.128	+8±2	56±4	4.80±0.55
(4,4)	0.882±0.215	–57±20	174±40	3.55±0.87

3. Results

Fig. 1 shows the measured spectra toward the central 0.5 kpc, displaying a velocity range between −530 and +350 km s^{-1}. Line parameters are given in Table 1. The (1,1) to (3,3) lines are clearly detected; the (4,4) line is observed at a 4.5σ level. The (1,1) to (3,3) profiles show two distinct velocity components, separated by ∼85 km s^{-1}. In the (1,1) and (2,2) lines, the higher velocity component is stronger; in the (3,3) line, however, both components show similar line strength. In the (4,4) transition it is difficult to resolve the two features but the line center is closer to the velocity of the –80 km s^{-1} component (Table 1). This is also suggested by a fit to the (4,4) line shown in Fig. 1, where 60–65% of the emission seems to arise from the –80 km s^{-1} component. We conclude that there is a trend with the –80 km s^{-1} component rising in relative strength with excitation above the ground state.

4. Determination of rotational temperatures

With hν/k ∼ 1.14 K and expected excitation temperatures $\gtrsim$10 K across an inversion doublet we obtain, in the optically thin case, beam averaged column densities of

$$N(J,K) = \frac{7.77 \cdot 10^{13}}{\nu}\ \frac{J(J+1)}{K^2}\ \int T_{\rm mb}\,{\rm d}v$$

for an individual inversion state. The column density N is in cm^{-2}, the frequency ν is in GHz. Calculated column densities are displayed in the last column of Table 1. For our observed metastable ($J = K$) inversion transitions, the rotational temperature $T_{\rm rot}$ between the states (J,J)

and (J', J') can then be obtained from

$$\frac{N(J,J)}{N(J',J')} = \frac{g_{\rm op}(J')}{g_{\rm op}(J)}\,\frac{2J'+1}{2J+1}\,\exp\left(\frac{-\Delta E}{{\rm k}\,T_{\rm rot}}\right),$$

where $g_{\rm op} = 1$ for para-ammonia, i.e. for $(J, K) = (1,1)$, (2,2), and (4,4), and $g_{\rm op} = 2$ for ortho-ammonia, i.e. for the (3,3) line. ΔE is the energy difference between the states involved.

Rotation diagrams of the ammonia emission in the (1,1) to (4,4) lines are shown in Fig. 2. The (3,3) line, although belonging to a different ammonia species, fits well in the general trend of decreasing normalized column density with energy above the ground state. The slope of the lines fitting the normalized column densities is $-\log {\rm e}/T_{\rm rot}$. A fit to the total ammonia emission (solid line) yields a rotational temperature of 85±15 K (1σ error). As sometimes observed in Galactic sources, the inclusion of higher excited inversion levels leads to higher rotational temperature estimates. This is indicated by the decreasing (negative) slope of the lines connecting the measured points. For the two velocity components, only including the (1,1) to (3,3) lines, $T_{\rm rot}$ = 85±5 ($V_{\rm LSR} = -80\,{\rm km\,s^{-1}}$) and 55±10 K ($V_{\rm LSR} = +6\,{\rm km\,s^{-1}}$). As already mentioned, the tentative decomposition of the $(J, K) = (4,4)$ line into two gaussian components (Fig. 1) suggests that 60–65% of the emission arises from the $-80\,{\rm km\,s^{-1}}$ component. This yields, including all measured lines, $T_{\rm rot}$ = 115±15 and 65±7 K for the -80 and $+6\,{\rm km\,s^{-1}}$ velocity components. Although the relative errors are larger when the (4,4) line is included, it seems that rotational temperature gradients exist not only in the overall spectra, but also in individual velocity components.

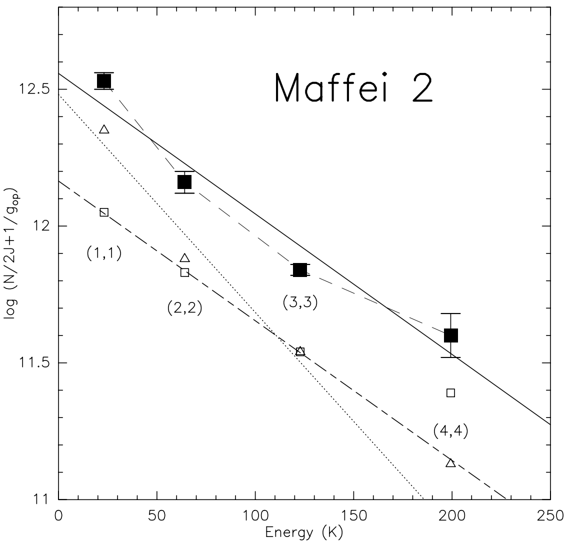

Fig. 2. A rotation diagram of metastable ammonia transitions towards Maffei 2, assuming optically thin emission and excitation temperatures ≫2.7 K for each inversion doublet. The column densities N from Table 1 refer to the upper state of the respective inversion doublet. Filled squares: Total emission (dashed lines connect the points); empty squares: $-80\,{\rm km\,s^{-1}}$ component; empty triangles: $+6\,{\rm km\,s^{-1}}$ component. Straight lines provide best fits to the total emission in the (J, K) = (1,1) – (4,4) lines (solid) and to the (1,1) – (3,3) emission lines for the -80 and $+6\,{\rm km\,s^{-1}}$ components (dashed and dotted, respectively). The decomposition of the (4,4) line into two velocity components is based on the fit shown in Fig. 1.

5. Discussion

5.1. Interpretation of rotational temperatures

The $J = K$ ammonia inversion doublets are called metastable because they decay radiatively via slow $\Delta K = \pm 3$ transitions. As a consequence, the relative population of these states is strongly affected by collisions and thus reflects (e.g. Walmsley & Ungerechts 1983) the kinetic temperature of the gas ($T_{\rm rot} \le T_{\rm kin}$).

One way to explain rising rotational temperatures with increasing energy above the ground state is the presence of kinetic temperature gradients. Alternatively, optically thick lines or subthermal excitation can produce the same effect (Goldsmith & Langer 1999). If the lines were thermalised to a given rotational temperature, but suffer from optical depth effects, our $T_{\rm rot}$ values would significantly underestimate actual $T_{\rm rot}$ values. Since these $T_{\rm rot}$ values would still be lower than $T_{\rm kin}$ and since differences between $T_{\rm rot}$ and $T_{\rm kin}$ may be substantial (e.g. Walmsley & Ungerechts 1983; Schilke 1989), this yields $T_{\rm kin} \gtrsim$ 200 K. Finally, radiative transfer calculations predict that rotational temperatures approach the kinetic temperature with rising energy of the analysed metastable inversion doublets. Again this yields rising $T_{\rm rot}$ with rising $E/{\rm k}$. To summarize: Independent of the interpretations outlined above, kinetic temperatures must be large ($T_{\rm kin} \gtrsim$ 100 K) and $T_{\rm kin}$ should be larger for the -80 than for the $+6\,{\rm km\,s^{-1}}$ velocity component.

5.2. A comparison with IC 342 and Galactic Center clouds

NH_3 integrated line temperatures are *larger* towards Maffei 2 than towards IC 342, also located at $D\sim$2.5 Mpc (Karachentsev et al. 1997). Emission from the inner 500 pc of the Milky Way would show similar intensities if observed from this distance (e.g. Hüttemeister et al. 1993a,b). From the (J, K) = (1,1) to (4,4) lines, $T_{\rm rot}\sim$85 K in Maffei 2, but only 50 K in IC 342 and the Galactic Center region.

Toward peak positions of clouds near the center of the Galaxy, (1,1) lines tend to be optically thick, while more highly excited inversion lines show no significant optical depth effects (Hüttemeister et al. 1993b). There are two main temperature components, one at $T_{\rm kin} \sim 25$ and one at $\sim$200 K. These, if present in Maffei 2 as well, could be responsible for the increasing rotational temperatures with E/k (Fig. 2). Such gradients are also seen in IC 342, if the (6,6) line is as strong as estimated from the tentative detection (see Martin & Ho 1986).

5.3. The nuclear region of Maffei 2

What kind of molecular gas is seen in ammonia? Critical densities, where collisional de-excitation matches spontaneous emission rates, are $n(\mathrm{H_2}) \sim 3{\cdot}10^3\mathrm{cm}^{-3}$ (e.g. Green 1980; Ho & Townes 1983). Our beam size (40″) matches the central bar with its size of 43″×9″ in ^{12}CO $J = 1$–0 (Ishiguro et al. 1989) and 40″×12″ in ^{13}CO $J = 1$–0 (Hurt & Turner 1991). The presence of bars provides a viable mechanism to transfer interstellar gas into the nuclear region of a galaxy, leading to the formation of dense molecular clouds and triggering bursts of star formation. As long as the gas is not yet fully ionized or swept away by stellar winds, it will coexist with the newly formed stars and will be heated by their radiation, by an enhanced flux of cosmic rays, by cloud-cloud collisions, and by the dissipation of turbulent energy. Both Maffei 2 and IC 342 show prominent nuclear bars and strong CO, infrared, and radio continuum emission (e.g. Lo et al. 1984; Ishiguro et al. 1989; Ishizuki et al. 1990; Hurt & Turner 1991; Turner & Ho 1994; Meier et al. 2000).

Assuming a grain emissivity law of λ^{-1}, dust temperatures deduced from the Kuiper Airborne Observatory and, for a larger region, from IRAS data (Rickard & Harvey 1983; IRAS 1989) are $T_{\mathrm{d}} = 33$–$47\,$K. Ignoring non-metastable inversion doublets, Table 1 implies that $N(\mathrm{NH_3})$ is on the order of $10^{14}\,\mathrm{cm}^{-2}$. For $\mathrm{H_2}$, with D=2.5 Mpc, $N(\mathrm{H_2}){\sim}10^{22}\,\mathrm{cm}^{-2}$ (Hurt & Turner 1991). This yields a relative abundance of $X(\mathrm{NH_3}){\sim}10^{-8}$. With $T_{\mathrm{rot}}(\mathrm{NH_3}) \gg T_{\mathrm{d}}$ and an unusually small $\mathrm{NH_3}$ abundance (e.g. Benson & Myers 1983; Brown et al. 1988), ammonia should trace a gas component that is different from that seen in CO (for an analysis of CO emission in a nuclear starburst environment, see Mao et al. 2000). Cloud-cloud collisions, young massive stars or ion-slip heating (Hüttemeister et al. 1993a,b) may cause the high rotational temperatures. SiO, an exclusive tracer of high temperature gas, was detected in Maffei 2 (Sage & Ziurys 1995) and is likely arising from the same gas component. Detailed studies of $\mathrm{NH_3}$ and SiO in the Galactic Center region (e.g. Hüttemeister et al. 1993a,b, 1998) indicate that the warm gas not directly associated with massive stars is only moderately dense ($n(\mathrm{H_2}){\sim}5{\cdot}10^3\mathrm{cm}^{-3}$).

From a comparison with the interferometric maps of Ishiguro et al. (1989) and Hurt & Turner (1991), the ammonia component at +6 kms must arise SW, the –80 km s^{-1} component NE of the center of the galaxy. Why is the rotation diagram (Fig. 2) indicating higher excitation NE of the nucleus? The bar in Maffei 2 may be caused by a merger with a satellite galaxy in the NE that severely disrupts this side of the galaxy (Hurt et al. 1996). This might have led to differences in inflow rates, star forming rates, and gas heating at the north-eastern and south-western sides of the nucleus. While our observed small scale (∼500 pc) nuclear asymmetry in rotational temperature may be consistent with the large scale asymmetry observed in HI, the proposed connection between these phenomena remains speculative. More data on the putative interacting dwarf galaxy, detailed simulations of the interaction, and models of the evolution of the nuclear bar are needed to verify or to reject the proposed scenario and to explain the recent past of Maffei 2.

References

Baars J.W.M., Genzel R., Pauliny-Toth I.I.K., Witzel A., 1977, A&A 61, 99
Benson P.J., Myers P.C., 1983, ApJ 270, 589
Brown P.D., Charnley S.B., Millar T.J., 1988, MNRAS 231, 409
Goldsmith P.F., Langer W.D., 1999, ApJ 517, 209
Green S., 1980, J. Chem. Phys. 73, 2740
Heikkilä A., Johansson L.E.B., Olofsson H., 1999, A&A 344, 817
Hermsen W., Wilson T.L., Walmsley C.M., Henkel C., 1988, A&A 201, 285
Ho P.T.P., Townes C.H., 1983, ARA&A 21, 239
Ho P.T.P., Martin R.N., Ruf K., 1982, A&A 113, 155
Ho P.T.P., Martin R.N., Turner J.L., Jackson J.M., 1990, ApJ 355, L19
Hurt R.L., Turner J.L., 1991, ApJ 377, 434
Hurt R.L., Turner J.L., Ho P.T.P., 1996, ApJ 466, 135
Hüttemeister S., Wilson T.L., Henkel C., Mauersberger R., 1993a, A&A 276, 445
Hüttemeister S., Wilson T.L., Bania T.M., Martín-Pintado J., 1993b, A&A 280, 255
Hüttemeister S., Mauersberger R., Henkel C., 1997, A&A 326, 59
Hüttemeister S., Dahmen G., Mauersberger R. et al., 1998, A&A 334, 646
IRAS Point Source Catalog, Cataloged Galaxies and Quasars observed in the IRAS Survey, Version 2.0, L. Fullmer & C. Lonsdale, 1989
Ishiguro M., Kawabe, R., Morita K.-I. et al., 1989, ApJ 344, 763
Ishizuki S., Kawabe R., Ishiguro M. et al., 1990, Nat 344, 224
Jackson J.M., Paglione T.A.D., Carlstrom J.E., Nguyen-Q-Rieu, 1995, ApJ 438, 695
Karachentsev I., Drozdovsky I., Kajsin S. et al., 1997, A&AS 124, 559
Lo K.-Y., Berge G.L., Claussen M.J. et al., 1984, ApJ 282, L59
Mao R.Q., Henkel C., Schulz A. et al., 2000, A&A 358, 433
Martin R.N., Ho P.T.P., 1979, A&A 74, L7
Martin R.N., Ho P.T.P., 1986, ApJ 308, L7
Mauersberger R., Henkel C., 1989, A&A 223, 79
Mauersberger R., Wilson T.L., Henkel C., 1988, A&A 201, 123
Mauersberger R., Henkel C., Sage L.J., 1990, A&A 236, 63
Meier D.S., Turner J.L., Hurt R.L., 2000, ApJ 531, 200
Ott M., Witzel A., Quirrenbach A. et al., 1994, A&A 284, 331
Paglione T.A.D., Jackson J.M., Ishizuki S., 1997, ApJ 484, 656
Rickard L.J., Harvey P.M., 1983, ApJ 268, L7
Sage L.J., Ziurys L.M., 1995, ApJ 447, 625
Schilke P., 1989, Diploma Thesis, Univ. of Bonn
Turner J.L., Ho P.T.P., 1994, ApJ 421, 122
Walmsley C.M., Ungerechts H., 1983, A&A 122, 164